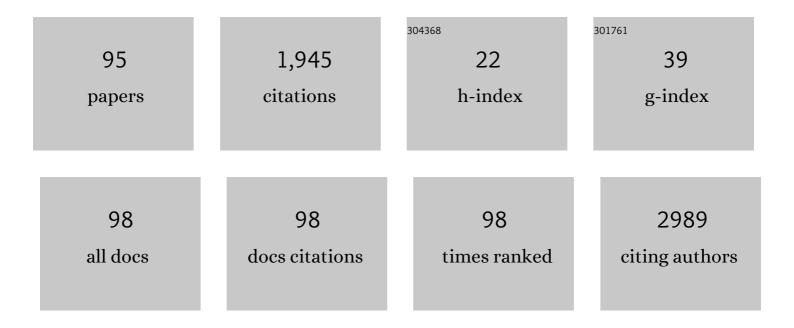
Oliver Bieri

List of Publications by Year in descending order

Source: https://exaly.com/author-pdf/5628654/publications.pdf Version: 2024-02-01



OLIVED RIEDI

#	Article	IF	CITATIONS
1	Nasal chondrocyte-based engineered autologous cartilage tissue for repair of articular cartilage defects: an observational first-in-human trial. Lancet, The, 2016, 388, 1985-1994.	6.3	214
2	Fundamentals of balanced steady state free precession MRI. Journal of Magnetic Resonance Imaging, 2013, 38, 2-11.	1.9	176
3	Quantitative muscle MRI: A powerful surrogate outcome measure in Duchenne muscular dystrophy. Neuromuscular Disorders, 2015, 25, 679-685.	0.3	88
4	Spinal cord volume loss. Neurology, 2018, 91, e349-e358.	1.5	66
5	Model-guided respiratory organ motion prediction of the liver from 2D ultrasound. Medical Image Analysis, 2014, 18, 740-751.	7.0	59
6	Matrix pencil decomposition of timeâ€resolved proton MRI for robust and improved assessment of pulmonary ventilation and perfusion. Magnetic Resonance in Medicine, 2017, 77, 336-342.	1.9	57
7	Novel magnetic resonance technique for functional imaging of cystic fibrosis lung disease. European Respiratory Journal, 2017, 50, 1701464.	3.1	57
8	Improved Muscle Function in Duchenne Muscular Dystrophy through L-Arginine and Metformin: An Investigator-Initiated, Open-Label, Single-Center, Proof-Of-Concept-Study. PLoS ONE, 2016, 11, e0147634.	1.1	50
9	Ultra-fast steady state free precession and its application to in vivo ¹ H morphological and functional lung imaging at 1.5 tesla. Magnetic Resonance in Medicine, 2013, 70, 657-663.	1.9	49
10	Combining phase images from array coils using a short echo time reference scan (COMPOSER). Magnetic Resonance in Medicine, 2017, 77, 318-327.	1.9	49
11	Quantitative in vivo diffusion imaging of cartilage using double echo steadyâ€state free precession. Magnetic Resonance in Medicine, 2012, 68, 720-729.	1.9	47
12	Preferential spinal cord volume loss in primary progressive multiple sclerosis. Multiple Sclerosis Journal, 2019, 25, 947-957.	1.4	44
13	Assessing White Matter Microstructure in Brain Regions with Different Myelin Architecture Using MRI. PLoS ONE, 2016, 11, e0167274.	1.1	37
14	The 6-minute walk test, motor function measure and quantitative thigh muscle MRI in Becker muscular dystrophy: A cross-sectional study. Neuromuscular Disorders, 2016, 26, 414-422.	0.3	36
15	Ultraâ€fast Steadyâ€State Free Precession Pulse Sequence for Fourier Decomposition Pulmonary MRI. Magnetic Resonance in Medicine, 2016, 75, 1647-1653.	1.9	36
16	Structural and Functional Lung Impairment in Primary Ciliary Dyskinesia. Assessment with Magnetic Resonance Imaging and Multiple Breath Washout in Comparison to Spirometry. Annals of the American Thoracic Society, 2018, 15, 1434-1442.	1.5	36
17	SSFP signal with finite RF pulses. Magnetic Resonance in Medicine, 2009, 62, 1232-1241.	1.9	34
18	Effect of Combination <scp>l</scp> -Citrulline and Metformin Treatment on Motor Function in Patients With Duchenne Muscular Dystrophy. JAMA Network Open, 2019, 2, e1914171.	2.8	34

#	Article	IF	CITATIONS
19	Ventilation and perfusion assessed by functional MRI in children with CF: reproducibility in comparison to lung function. Journal of Cystic Fibrosis, 2019, 18, 543-550.	0.3	32
20	Quantitative mapping of <i>T</i> ₂ using partial spoiling. Magnetic Resonance in Medicine, 2011, 66, 410-418.	1.9	30
21	A comparison of multi-echo spin-echo and triple-echo steady-state T2 mapping for in vivo evaluation of articular cartilage. European Radiology, 2016, 26, 1905-1912.	2.3	28
22	Timed function tests, motor function measure, and quantitative thigh muscle MRI in ambulant children with Duchenne muscular dystrophy: A cross-sectional analysis. Neuromuscular Disorders, 2018, 28, 16-23.	0.3	28
23	Tamoxifen in Duchenne muscular dystrophy (TAMDMD): study protocol for a multicenter, randomized, placebo-controlled, double-blind phase 3 trial. Trials, 2019, 20, 637.	0.7	27
24	Variable flip angle T ₁ mapping in the human brain with reduced t ₂ sensitivity using fast radiofrequencyâ€spoiled gradient echo imaging. Magnetic Resonance in Medicine, 2016, 75, 1413-1422.	1.9	25
25	Motion-insensitive rapid configuration relaxometry. Magnetic Resonance in Medicine, 2017, 78, 518-526.	1.9	22
26	Longitudinal 2-point dixon muscle magnetic resonance imaging in becker muscular dystrophy. Muscle and Nerve, 2015, 51, 918-921.	1.0	21
27	Rapid 3D in vivo 1H human lung respiratory imaging at 1.5 T using ultraâ€fast balanced steadyâ€state free precession. Magnetic Resonance in Medicine, 2017, 78, 1059-1069.	1.9	19
28	MRI characteristics of supraclavicular brown adipose tissue in relation to coldâ€induced thermogenesis in healthy human adults. Journal of Magnetic Resonance Imaging, 2019, 50, 1160-1168.	1.9	19
29	Functional lung imaging with transient spoiled gradient echo. Magnetic Resonance in Medicine, 2019, 81, 1915-1923.	1.9	19
30	Suitability of Magnetic Resonance Imaging for Guided Endodontics: Proof of Principle. Journal of Endodontics, 2021, 47, 954-960.	1.4	19
31	Imaging of Primary Brain Tumors and Metastases with Fast Quantitative 3â€Dimensional Magnetization Transfer. Journal of Neuroimaging, 2015, 25, 1007-1014.	1.0	18
32	Ultrafast 3D balanced steadyâ€state free precession MRI of the lung: Assessment of anatomic details in comparison to lowâ€dose CT. Journal of Magnetic Resonance Imaging, 2015, 42, 602-609.	1.9	17
33	The comparison of the performance of 3†T and 7†T T2 mapping for untreated low-grade cartilage lesions. Magnetic Resonance Imaging, 2019, 55, 86-92.	1.0	17
34	Longitudinal reliability of outcome measures in patients with Duchenne muscular dystrophy. Muscle and Nerve, 2020, 61, 63-68.	1.0	17
35	Steady state free precession magnetization transfer imaging. Magnetic Resonance in Medicine, 2008, 60, 1261-1266.	1.9	16
36	The impact of segmentation on wholeâ€lung functional MRI quantification: Repeatability and reproducibility from multiple human observers and an artificial neural network. Magnetic Resonance in Medicine, 2021, 85, 1079-1092.	1.9	16

#	Article	IF	CITATIONS
37	Synchronous MRI of muscle motion induced by electrical stimulation. Magnetic Resonance in Medicine, 2017, 77, 664-672.	1.9	15
38	Spinal cord imaging using averaged magnetization inversion recovery acquisitions. Magnetic Resonance in Medicine, 2018, 79, 1870-1881.	1.9	15
39	Hybrid ultrasound―MR guided HIFU treatment method with 3 D motion compensation. Magnetic Resonance in Medicine, 2018, 79, 2511-2523.	1.9	15
40	3.0 T MR imaging of the ankle: Axial traction for morphological cartilage evaluation, quantitative T2 mapping and cartilage diffusion imaging—A preliminary study. European Journal of Radiology, 2015, 84, 1546-1554.	1.2	14
41	Quantification of Liver, Subcutaneous, and Visceral Adipose Tissues by MRI Before and After Bariatric Surgery. Obesity Surgery, 2019, 29, 2795-2805.	1.1	14
42	On the fluidâ€tissue contrast behavior of highâ€resolution steadyâ€state sequences. Magnetic Resonance in Medicine, 2012, 68, 1586-1592.	1.9	13
43	7 Tesla quantitative hip MRI: a comparison between TESS and CPMG for T2 mapping. Magnetic Resonance Materials in Physics, Biology, and Medicine, 2016, 29, 503-512.	1.1	13
44	Threeâ€dimensional oxygenâ€enhanced <scp>MRI</scp> of the human lung at 1.5 <scp>T</scp> with ultraâ€fast balanced steadyâ€state free precession. Magnetic Resonance in Medicine, 2018, 79, 246-255.	1.9	13
45	The Neural Mechanisms of Associative Memory Revisited: fMRI Evidence from Implicit Contingency Learning. Frontiers in Psychiatry, 2019, 10, 1002.	1.3	13
46	Generation and characterization of osteochondral grafts with human nasal chondrocytes. Journal of Orthopaedic Research, 2015, 33, 1111-1119.	1.2	12
47	Balanced steadyâ€state free precession thoracic imaging with halfâ€radial dualâ€echo readout on smoothly interleaved archimedean spirals. Magnetic Resonance in Medicine, 2020, 84, 237-246.	1.9	12
48	Impact of internal target volume definition for pencil beam scanned proton treatment planning in the presence of respiratory motion variability for lung cancer: A proof of concept. Radiotherapy and Oncology, 2020, 145, 154-161.	0.3	12
49	Pulmonary relaxometry with inversion recovery ultraâ€fast steadyâ€state free precession at 1.5T. Magnetic Resonance in Medicine, 2017, 77, 74-82.	1.9	10
50	Simultaneous multislice tripleâ€echo steadyâ€state (<scp>SMSâ€TESS</scp>) T ₁ , T ₂ , PD, and offâ€resonance mapping in the human brain. Magnetic Resonance in Medicine, 2018, 80, 1088-1100.	1.9	10
51	Automatic Spinal Cord Gray Matter Quantification: A Novel Approach. American Journal of Neuroradiology, 2019, 40, 1592-1600.	1.2	10
52	Orientation dependence and decay characteristics of T ₂ * relaxation in the human meniscus studied with 7 Tesla MR microscopy and compared to histology. Magnetic Resonance in Medicine, 2019, 81, 921-933.	1.9	10
53	Comparison of [18F]FDG PET/CT with magnetic resonance imaging for the assessment of human brown adipose tissue activity. EJNMMI Research, 2020, 10, 85.	1.1	10
54	Fast Open-Source Toolkit for Water T2 Mapping in the Presence of Fat From Multi-Echo Spin-Echo Acquisitions for Muscle MRI. Frontiers in Neurology, 2021, 12, 630387.	1.1	9

#	Article	IF	CITATIONS
55	Liver-ultrasound based motion modelling to estimate 4D dose distributions for lung tumours in scanned proton therapy. Physics in Medicine and Biology, 2020, 65, 235050.	1.6	9
56	MRI Shows Lung Perfusion Changes after Vaping and Smoking. Radiology, 2022, 304, 195-204.	3.6	9
57	True constructive interference in the steady state (trueCISS). Magnetic Resonance in Medicine, 2018, 79, 1901-1910.	1.9	8
58	Liver-ultrasound-guided lung tumour tracking for scanned proton therapy: a feasibility study. Physics in Medicine and Biology, 2021, 66, 035011.	1.6	8
59	An analytical description of balanced steady-state free precession with finite radio-frequency excitation. Magnetic Resonance in Medicine, 2011, 65, 422-431.	1.9	7
60	Measurements of Motor Function and Other Clinical Outcome Parameters in Ambulant Children with Duchenne Muscular Dystrophy. Journal of Visualized Experiments, 2019, , .	0.2	7
61	Defect distribution index: A novel metric for functional lung MRI in cystic fibrosis. Magnetic Resonance in Medicine, 2021, 86, 3224-3235.	1.9	7
62	Synthetic 4DCT(MRI) lung phantom generation for 4D radiotherapy and image guidance investigations. Medical Physics, 2022, 49, 2890-2903.	1.6	7
63	Comparison between balanced steady-state free precession and standard spoiled gradient echo magnetization transfer ratio imaging in multiple sclerosis: methodical and clinical considerations. NeuroImage, 2015, 108, 87-94.	2.1	6
64	Reversed half-echo stack-of-stars TrueFISP (TrueSTAR). Magnetic Resonance in Medicine, 2016, 76, 583-590.	1.9	6
65	Simultaneous B 1 and T 1 mapping using spiral multislice variable flip angle acquisitions for wholeâ€brain coverage in less than one minute. Magnetic Resonance in Medicine, 2019, 81, 1876-1889.	1.9	6
66	Spinal cord gray matter atrophy is associated with functional decline in postâ€polio syndrome. European Journal of Neurology, 2022, 29, 1435-1445.	1.7	6
67	Dynamic and steadyâ€state oxygenâ€dependent lung relaxometry using inversion recovery ultraâ€fast steadyâ€state free precession imaging at 1.5 T. Magnetic Resonance in Medicine, 2018, 79, 839-845.	1.9	5
68	Dynamic MR imaging of the skeletal muscle in young and senior volunteers during synchronized minimal neuromuscular electrical stimulation. Magnetic Resonance Materials in Physics, Biology, and Medicine, 2020, 33, 393-400.	1.1	5
69	Normalization of Spinal Cord Total Cross-Sectional and Gray Matter Areas as Quantified With Radially Sampled Averaged Magnetization Inversion Recovery Acquisitions. Frontiers in Neurology, 2021, 12, 637198.	1.1	5
70	Quantification and Monitoring of the Effect of Botulinum Toxin A on Paretic Calf Muscles of Children With Cerebral Palsy With MRI: A Preliminary Study. Frontiers in Neurology, 2021, 12, 630435.	1.1	5
71	Effect of Salbutamol on Lung Ventilation in Children with Cystic Fibrosis: Comprehensive Assessment Using Spirometry, Multiple-Breath Washout, and Functional Lung Magnetic Resonance Imaging. Respiration, 2022, 101, 281-290.	1.2	5
72	Transverse Relaxation Anisotropy of the Achilles and Patellar Tendon Studied by <scp>MR</scp> Microscopy. Journal of Magnetic Resonance Imaging, 2022, 56, 1091-1103.	1.9	5

#	Article	IF	CITATIONS
73	Feasibility of Flat Panel Detector CT in Perfusion Assessment of Brain Arteriovenous Malformations: Initial Clinical Experience. American Journal of Neuroradiology, 2017, 38, 735-739.	1.2	4
74	Pure balanced steadyâ€state free precession imaging (pureÂbSSFP). Magnetic Resonance in Medicine, 2022, 87, 1886-1893.	1.9	4
75	MRI lung lobe segmentation in pediatric cystic fibrosis patients using a recurrent neural network trained with publicly accessible CT datasets. Magnetic Resonance in Medicine, 2022, 88, 391-405.	1.9	4
76	Rapid and robust variable flip angle T1mapping using interleaved two-dimensional multislice spoiled gradient echo imaging. Magnetic Resonance in Medicine, 2017, 77, 1606-1611.	1.9	3
77	Snapshot wholeâ€brain T ₁ relaxometry using steadyâ€state prepared spiral multislice variable flip angle imaging. Magnetic Resonance in Medicine, 2018, 79, 856-866.	1.9	3
78	OpenForce <scp>MR</scp> : A lowâ€cost openâ€source MRâ€compatible force sensor. Concepts in Magnetic Resonance Part B, 2018, 48B, .	0.3	3
79	Imaging of the thoracic spinal cord using radially sampled averaged magnetization inversion recovery acquisitions. Journal of Neuroscience Methods, 2020, 343, 108825.	1.3	3
80	On the optimal temporal resolution for phase contrast cardiovascular magnetic resonance imaging: establishment of baseline values. Journal of Cardiovascular Magnetic Resonance, 2020, 22, 72.	1.6	3
81	Ultrasound-driven cardiac MRI. Physica Medica, 2020, 70, 161-168.	0.4	3
82	Configurationâ€based electrical properties tomography. Magnetic Resonance in Medicine, 2021, 85, 1855-1864.	1.9	3
83	Dynamic MRI of plantar flexion: A comprehensive repeatability study of electrical stimulation-gated muscle contraction standardized on evoked force. PLoS ONE, 2020, 15, e0241832.	1.1	3
84	assessment of time dependent changes of T2* in medial meniscus under loading at 3T: A preliminary study. Journal of Applied Biomedicine, 2018, 16, 138-144.	0.6	3
85	Free-breathing half-radial dual-echo balanced steady-state free precession thoracic imaging with wobbling Archimedean spiral pole trajectories. Zeitschrift Fur Medizinische Physik, 2023, 33, 220-229.	0.6	3
86	Signal enhancement ratio imaging of the lung parenchyma with ultraâ€fast steadyâ€state free precession MRI at 1.5T. Journal of Magnetic Resonance Imaging, 2018, 48, 48-57.	1.9	2
87	Superbalanced steady state free precession. Magnetic Resonance in Medicine, 2012, 67, 1346-1354.	1.9	1
88	Oneâ€minute wholeâ€brain magnetization transfer ratio imaging with intrinsic B 1 â€correction. Magnetic Resonance in Medicine, 2021, 85, 2686-2695.	1.9	1
89	Variable echo time imaging for detecting the short T2* components of the sciatic nerve: a validation study. Magnetic Resonance Materials in Physics, Biology, and Medicine, 2021, 34, 411-419.	1.1	1
90	Treatment with Lâ€Citrulline in patients with postâ€polio syndrome: A single center, randomized, double blind, placeboâ€controlled trial. Neuromuscular Disorders, 2021, 31, 1136-1143.	0.3	1

#	Article	IF	CITATIONS
91	Complex B 1 + mapping with Carrâ€Purcell spin echoes and its application to electrical properties tomography. Magnetic Resonance in Medicine, 2021, , .	1.9	1
92	Pretreatment Normal WM Magnetization Transfer Ratio Predicts Risk of Radiation Necrosis in Patients with Medulloblastoma. American Journal of Neuroradiology, 2022, 43, 299-303.	1.2	1
93	An analytical description of balanced steady-state free precession with finite radio-frequency excitation. Magnetic Resonance in Medicine, 2011, 65, spcone-spcone.	1.9	Ο
94	Cardiovascular magnetization transfer ratio imaging compared with histology: A postmortem study. Journal of Magnetic Resonance Imaging, 2014, 40, spcone-spcone.	1.9	0
95	Signal enhancement ratio imaging of the lung parenchyma with ultra-fast steady-state free precession MRI at 1.5T. Journal of Magnetic Resonance Imaging, 2018, 48, spcone-spcone.	1.9	0